Single-walled carbon nanotubes-chitin based saturable absorber for enhanced 1.5-micron Q-switching laser generation

NUR NASYITAH MD RAHIM[1], SITI NUR FATIN ZUIKAFLY[1], SULAIMAN WADI HARUN[2], HAFIZAL YAHAYA[1], FAUZAN AHMAD[1,*]
[1]*Malaysia-Japan International Institute of Technology, Universiti Teknologi Malaysia, Jalan Sultan Yahya Petra, 54100 Kuala Lumpur, Malaysia*
[2] *Photonics Engineering Laboratory, Department of Electrical Engineering, Faculty of Engineering, University of Malaya, 50603 Kuala Lumpur, Malaysia*

In order to produce Q-switched laser pulses, this study sought to illustrate and assess the synergistic effect of passive saturable absorber (SA) based on single-walled carbon nanotubes (SWCNT) in chitin as the host polymer. This work describes the use of SWCNT-chitin SA to generate a Q-switched pulsed laser that operates at 1530.61 nm. The SWCNT-chitin achieved a highest repetition rate of 154.80 kHz and shortest pulse width of 2.34 μs, at maximum input pump power of 273.52 mW. This study highlights chitin as a promising natural host polymer, offering a compelling alternative to synthetics polymers such as polyvinyl alcohol (PVA), and polyethylene oxide (PEO).

(Received October 9, 2024; accepted June 4, 2025)

Keywords: Saturable absorber, Single-walled carbon nanotubes, Chitin, Q-switched, Erbium-doped fiber laser

1. Introduction

The quest for advanced Q-switched lasers operating in 1.5-micron region has been driven by their indispensable role in modern telecommunications, and sensing applications [1–3]. This wavelength regime, facilitated by erbium-doped fiber lasers (EDFL), enabling efficient long-distance data transmission and remote sensing capabilities crucial for our interconnected world. At the heart of these laser systems lies the saturable absorber, a key component pivotal in achieving stable and high-energy pulsed outputs essential for diverse technological applications.

The convergence of cutting-edge materials science and photonics has spotlighted single walled carbon nanotubes (SWCNTs) as exceptionally promising materials for saturable absorbers. Their remarkable nonlinear optical properties, including ultrafast response times and high optical damage thresholds, position them as prime candidates for enhancing laser performance [4,5]. In the field of pulsed fiber laser, the incorporations of the materials including SWCNT into polymer matrices has been widely utilized to create polymer-composite-based SA. This approach enhances handling and mechanical tolerance which is beneficial in laser generation applications [6–9]. Synthetic polymer such as polyvinyl alcohol (PVA) and polyethylene oxide (PEO) have been extensively studied for SA applications. For instance, Mafroos et al. [10], investigated the use of SWCNTs in a PVA host polymer for Q-switching in an EDFL. They obtained a stable Q-switched laser with repetition rate of 130 kHz, pulse width of 3.62 μs, and pulse energy of 12.24 nJ. On the other hand, Ahmed et al. [11], utilized multiwalled-carbon nanotubes (MWCNT) embedded in PEO as host polymer. They observed a self-starting Q-switched pulsed laser operating at 1533.60 nm with the repetition rate of 33.62 kHz, pulse width of 4.2 μs and highest pulse energy of 531 nJ.

However, these polymers often suffer from poor environmental stability and low melting points, which decreases the damage threshold of the SA [12]. Concurrently, natural polymers such as chitin have emerged as sustainable alternatives for hosting and stabilizing CNTs. Derived from abundant marine sources, chitin boasts inherent biocompatibility, mechanical robustness, biodegradability, and low toxicity, making it an ideal matrix material for various optoelectronic applications [13–15]. Integrating SWCNT within a chitin matrix leveraged on these advantages offered by chitin as host polymer. This combination not only enhances the stability and efficiency of Q-switched lasers but also opens avenues for sustainable and bio-compatible photonics applications. Zuikafly et al. [13]was the first to demonstrate the applicability of chitin as host polymer with graphene as nanomaterials. They obtained the shortest pulse width of 1.33 μs, repetition rate of 111.77 kHz and pulse energy of 14.37 nJ.

This paper delves into the innovative use of single-walled carbon nanotube (SWCNT)-chitin composite films as advanced saturable absorbers within EDFL cavities operating specifically at the critical 1.5-micron wavelength. We meticulously explore the performance evaluations of these novel composite materials. Emphasis is placed on elucidating how the integration of SWCNTs within the chitin matrix not only augments the nonlinear optical response but also ensures seamless compatibility within the

demanding EDFL cavity environment. Therefore, this research not only advances the fundamental understanding of SWCNT-chitin composites but also paves the way for practical implementations in ultrafast photonics and beyond, promising significant strides in the development of next-generation laser technologies.

2. Method overview

2.1. SWCNT-chitin SA fabrication and characterization

The SWCNT-based SA was fabricated using single-walled carbon nanotubes with the purity of 99%, purchased from Cheap Tubes Inc. The SWCNT had diameters of 1 to 2 nm and lengths of 3 to 30 µm. The SWCNT solution was prepared by dispersing 250 mg of SWCNT powder into 1% SDS solution with a molecular weight of 288.28 g/mol from Sigma Aldrich. The mixture underwent ultrasonic treatment using a tip sonicator (Q500 Qsonica) operating at 20 kHz with an amplitude of 40% programmed to cycle with pulses of 30 seconds "ON" and 10 seconds "OFF" for a total duration of 3 hours. Following sonication, the suspension was centrifuged at 1000 rpm for 1 hour at a controlled room temperature of 25 ± 2 °C. The purpose of this step is to remove the aggregated portions of the SWCNT. The SWCNT was then suspended in chitin as the host polymer to form a film.

The preparation of chitin solution was adopted based on previous study by Nawawi et al. [16]. The preparation commenced with the thawing and rinsing of Pleurotus ostreatus mushrooms with distilled water for 5 minutes to eliminate visible contaminants. Following three washes, the mushrooms were blended for 5 minutes using a commercial kitchen blender. An extraction process was conducted using hot water at 85°C for 30 minutes. At this stage, the excess water containing the water-soluble components was removed from the extract via centrifugation process. The residual extract was then soaked in 1 M sodium hydroxide (NaOH) to strip away proteins, lipids, and alkaline-soluble polysaccharides. The mixture was re-centrifuged to eliminate excess solids, diluted in water (0.8% w/v), and stored in 4°C until further use. In order to prepare the SWCNT-chitin SA, the SWCNT suspension was combined with the chitin solution in a one-to-one ratio. Following another round of centrifugation for 60 minutes, the solution was then transferred to a petri dish and left to dry for 48 hours at room temperature, resulting in a free-standing SWCNT-chitin SA film.

Prior to evaluating the generated pulsed laser performance, the fabricated film's thickness was measured using a 3D measuring laser microscope (LEXT OLS4100, Olympus). The film thickness was measured at three distinct points, and the average thickness, as depicted in Fig. 1, was calculated to be 68.91 µm, aligning with the suggested range [17,18]. The regions with non-uniform thickness, as showed in Fig. 1, was excluded from further characterization.

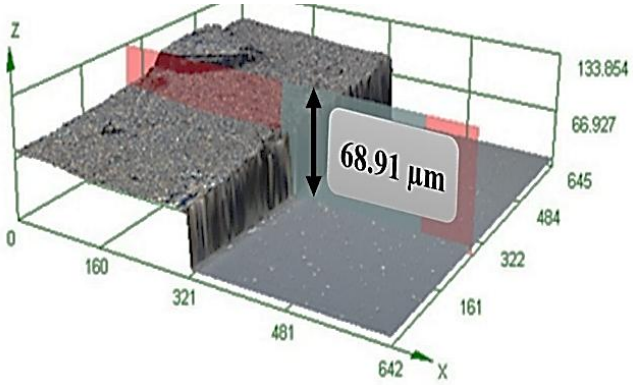

Fig. 1. The thickness measurement of SWCNT-chitin SA (colour online)

In addition, the morphological structure of the fabricated film was also assessed using a low-vacuum scanning electron microscopy (LVSEM) (JSM-IT300, JEOL). Surface morphology analysis was conducted at 1000x magnification with an accelerating voltage of 5 kV. The morphological characterization of polymers using LVSEM often presents challenges due to their susceptibility to electron beam damage [19]. To mitigate this issue, the SA film was coated with platinum (Pt) via an auto fine sputter coater (JEC-300FC, JEOL). As illustrated in Fig. 2, the SWCNT-chitin SA exhibits a uniform surface morphology at 1000x magnifications, devoid of visible holes or pitting which is crucial for the SA performance. The surface exhibits rough elephant skin-like surface and string-like structure indicating the amorphous structure of the glucans that holds the dense network of fibres [20].

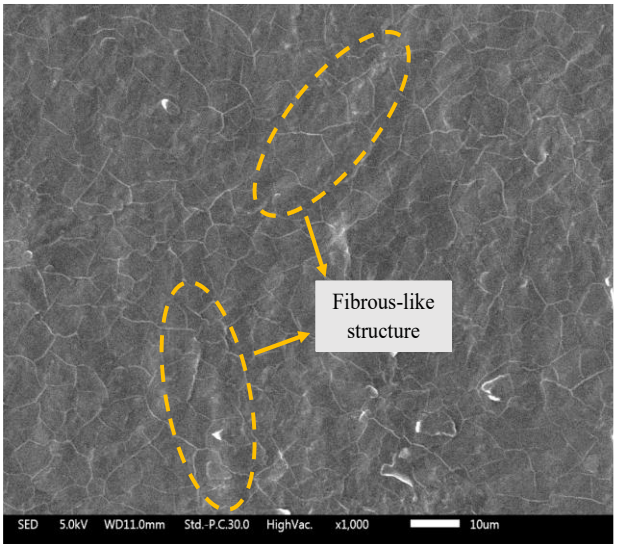

Fig. 2. Surface morphology of SWCNT-chitin SA at 1000x magnifications (colour online)

2.2. Q-Switching laser configuration using EDFL cavity

Fig. 3 depicts the configuration of the EDFL with CNT-PVA-based saturable absorber (SA) used in this study.

Pulse generation at the 1.5 μm wavelength was achieved using a 1.5 m EDFL as the gain medium in the laser cavity. The ring cavity consisted of 980 nm laser diode pump coupled through a 980/1550 nm wavelength division multiplexer (WDM). The output signal was tapped out using a 80/20 output coupler, directing 80% of the pulses to remain within the cavity for continuous oscillation, while the remaining 10% was utilized for output measurement to observe for the pulse performance concurrently. An optical isolator was placed after the gain medium to ensure there is no backflow of the generated pulses. The output signal characteristics were monitored using a 350 MHz oscilloscope (GDS 3501, GWINSTEK), an optical spectrum analyzer (OSA) (AG6370B Yokogawa), and a radio frequency spectrum analyzer (RFSA) (MS2830A Anritsu).

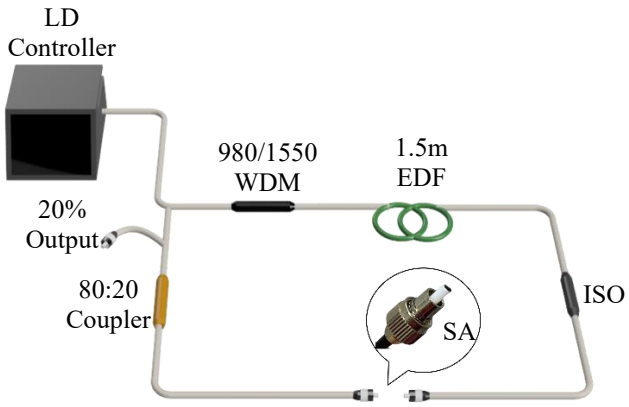

Fig. 3. The schematic diagram of the Q-switching laser configuration using EDFL (colour online)

3. Results and discussion

The fabricated SWCNT-chitin SA was integrated into an EDFL cavity by sandwiching it between two fiber end facets, as depicted in Fig. 3. To investigate the performance of the generated pulsed laser, we varied the pump power and closely monitor the output signal. Upon reaching a threshold pump power of 57.15 mW, the EDFL began to generate stable Q-switching pulses. However, when the pump power was increased beyond 273.52 mW, the pulse signal was fully diminished due to the over-saturation of the SA at such high intensities. Interestingly, the pulse signal could be recovered by maintaining the pump power within the range of 57.15 to 273.52 mW. Throughout this range, no thermal damage was observed on the SA, demonstrating that the film was robust enough to withstand the high-power levels without degradation. This is owing to the high thermal damage of the chitin compared to synthetic polymers such as PEO and PVA [21,22].

Fig. 4 illustrates the optical spectrum traces for the continuous wave (CW) operation in comparison to the operation with the SWCNT-chitin SA integrated into the cavity. In CW mode, the laser operated at a wavelength of 1559.84 nm. However, when the SA was inserted, the wavelength shifted to a shorter wavelength of 1530.61 nm. This shift can be attributed to the additional loss introduced by the SA within the cavity. To compensate for this loss, the oscillating wavelength shortened, indicating the dynamic interaction between the SA and the laser cavity [23]. By methodically varying the pump power and observing the corresponding laser performance, it became evident that the SWCNT-chitin SA not only facilitated stable Q-switching pulses but also maintained structural integrity under high power conditions. The wavelength shift underscores the nuanced influence of the SA on the laser's operational characteristics.

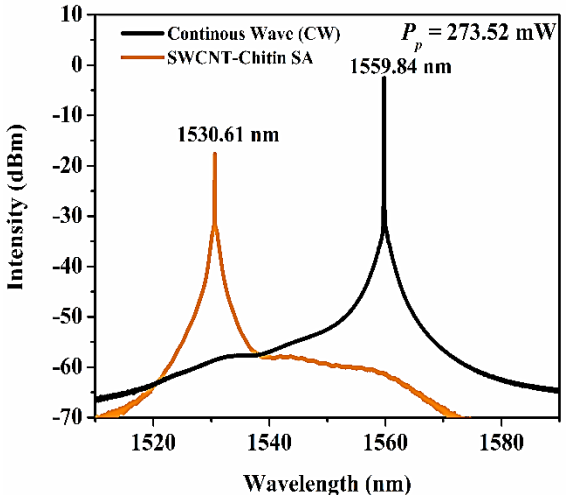

Fig. 4. Optical spectrum trace at maximum pump power of 273.52 mW for continuous wave (CW) and SWCNT-chitin SA (colour online)

Fig. 5 presents the pulse train captured at the peak pump power of 273.50 mW. The SWCNT-chitin SA exhibited a repetition rate of 154.80 kHz, with a pulse-to-pulse separation of 6.46 μs, as illustrated in Fig. 5. Additionally, the pulse's full width at half maximum (FWHM) was measured at 2.34 μs, as depicted in Fig. 6.

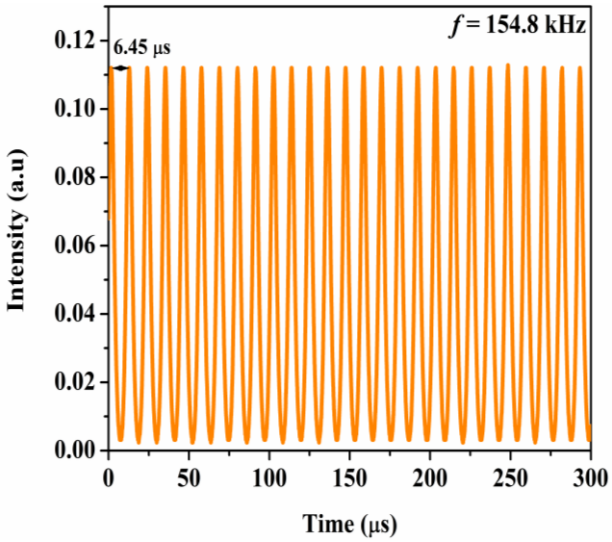

Fig. 5. Pulse train of Q-switched EDFL with repetition rate of 154.8 kHz (colour online)

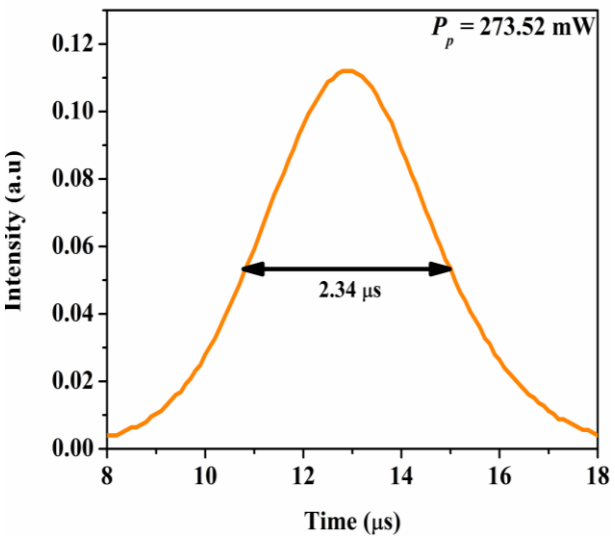

Fig. 6. Single pulse envelope of Q-switched EDFL with pulse width of 2.34 µs (colour online)

Fig. 7 illustrates the variations in Q-switching pulses as a function of pump power. Unlike mode-locking, where the repetition rate is typically fixed, the repetition rate of a Q-switched fiber laser is directly influenced by the intensity of the input pump power. As the pump power is adjusted from 57.15 to 273.52 mW, the repetition rate increases almost linearly—a behaviour commonly observed in Q-switched pulsed lasers, as noted in numerous studies. The pulse generation mechanism is driven by the saturation of the SA, leading to a higher repetition rate with increasing pump power. From Fig. 7, it is evident that both the repetition rate and pulse width are tuneable within specific ranges: the repetition rate can be adjusted from 90.04 kHz to 154.80 kHz, and the pulse width can be varied from 3.90 µs to 2.34 µs by changing the pump power from 57.15 to 273.52 mW. The wide range of pump power tunability can be linked to the concentration of SWCNT within the SA, enabling for enhanced level of saturation, and delays the SA bleaching process. This augmentation facilitates broader control over input power levels, optimizing conditions for efficient laser operation. The obtained repetition rate in this study was higher in comparison to the study by Zuikafly et al. [13], which was 111.77 kHz. This could be attributed to the SWCNT itself as SWCNT provides better performance in terms of the repetition rate in comparison to graphene [10].

In tandem with these changes, both the pulse energy and peak power exhibit an upward trend as the pump power increases, as depicted in Fig. 8. At the maximum pump power, the peak power reaches 9 mW, while the pulse energy is recorded at 21 nJ. This behaviour highlights the dynamic relationship between pump power and laser output characteristics, showcasing the tunability and efficiency of the Q-switched laser system. Nevertheless, the repetition rate and pulse energy obtained in this study is higher compared to previous study [10,13]. However, in comparison to the study conducted by Ahmed et al. [11], where MWCNT/PVA based SA was used, the pulse energy in this study is lower. This is owing to the thicker layer of the MWCNT compared to SWCNT, which allows for more absorption.

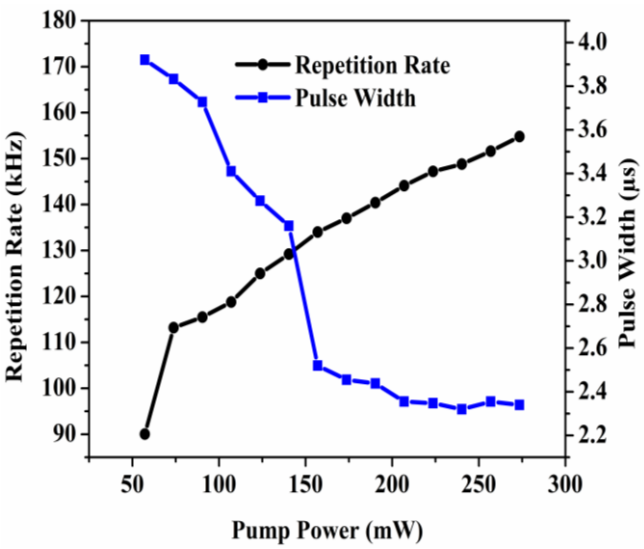

Fig. 7. Repetition rate and pulse width vs the input pump power (colour online)

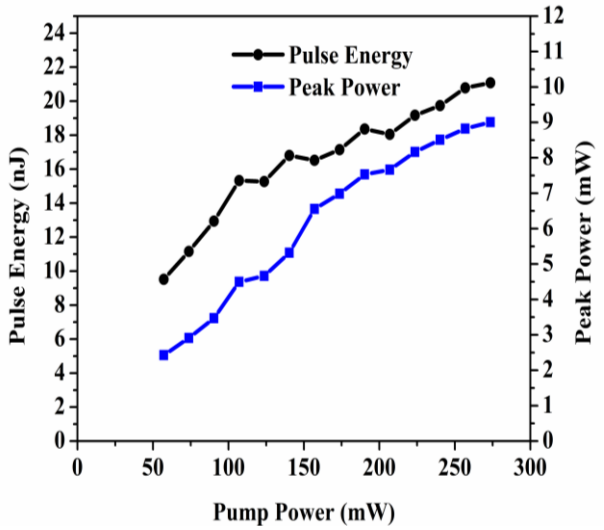

Fig. 8. Peak power and pulse energy vs the input pump power (colour online)

Furthermore, the stability of the pulsed laser output was assessed by analysing its radio frequency (RF) spectrum using a dedicated radio frequency spectrum analyser (RFSA). The findings indicated that the fundamental frequency recorded on the RFSA, 154.80 kHz, correlates closely with the peak-to-peak duration observed on the oscilloscope. Additionally, the fabricated SA exhibited a robust signal-to-noise ratio (SNR) of 48.65 dB, as evidenced in Fig. 9, affirming the consistency and reliability of the generated pulses without any signal irregularities.

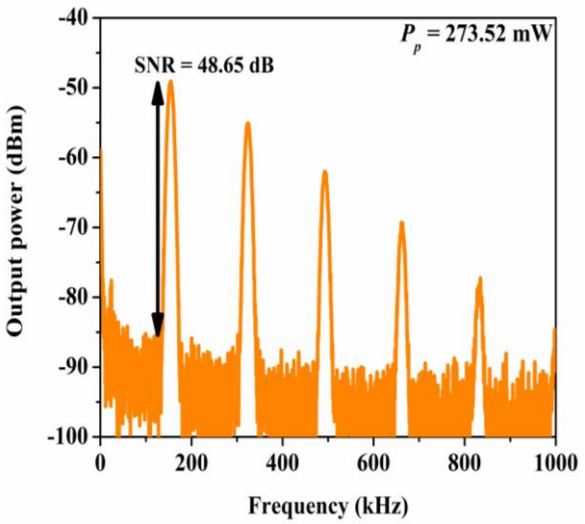

Fig. 9. RFSA measurement of SWCNT-chitin SA at maximum pump power (colour online)

4. Conclusion

In conclusion, we successfully achieved a stable and self-starting Q-switched laser in an EDFL using SWCNT-chitin as the saturable absorber. Our research demonstrated that the SWCNT-chitin SA, operating at 1530.61 nm, generated Q-switched pulses with an impressive repetition rate of 154.80 kHz and a pulse width of 2.34 µs. Additionally, the SA exhibited a high thermal damage threshold, withstanding a maximum input power of 273.52 mW. These findings highlight chitin's potential as a promising natural host polymer, enhancing the performance of incorporated materials like SWCNTs and offering a compelling alternative for advanced laser applications.

References

[1] M. M. Mafroos, N. Ameelia, H. H. Jameela, A. Hamzah, International Journal of Integrated Engineering **15**(3), 170 (2023).
[2] S. N. F. Zuikafly, H. Ahmad, M. F. Ismail, M. A. Abdul Rahman, W. J. Yahya, N. Abu Husain, K. A. Abu Kassim, H. Yahaya, F. Ahmad, Micromachines **14**(5), 1048 (2023).
[3] O. W. Ling, A. Hamzah, N. Mohamed, M. M. Mafroos, 4th International Conference on Smart Sensors and Application: Digitalization for Societal Well-Being, ICSSA 2022.
[4] D. Kang, S. Sarkar, K. S. Kim, S. Kim, Highly Nanoscale Research Letters **17**(1), 11 (2022).
[5] X. T. Xu, J. P. Zhai, J. S. Wang, Y. P. Chen, Y. Q. Yu, M. Zhang, I. L. Li; S. C. Ruan; Z. K. Tang, Applied Physics Letters, **104**(17), 171107 (2014).
[6] K. Y. Lau, D. Hou, Optics and Laser Technology **137**, 106826 (2021).
[7] S. A. Hussain, Scientific Reports **9**(1), 17282 (2019).
[8] F. Wang, A. G. Rozhin, Z. Sun, V. Scardaci, R. V. Penty, I. H. White, A. C. Ferrari, International Journal of Material Forming **1**(2), 107 (2008).
[9] N. A. El-Zaher, W. G. Osiris, Journal of Applied Polymer Science **96**(5), 1914 (2005).
[10] M. M. Mafroos, H. H. Jameela Sapingi, A. B. Hamzah, Indonesian Journal of Electrical Engineering and Computer Science **28**(1), 227 (2022).
[11] M. H. M. Ahmed, N. M. Ali, Z. S. Salleh, A. A. Rahman, S. W. Harun, M. Manaf, H. Arof, Optics and Laser Technology **65**, 25 (2015).
[12] T. Hasan, Z. Sun, F. Wang, F. Bonaccorso, P. H. Tan, A. G. Rozhin, A. C. Ferrari, Advanced Materials **21**(38-39), 3874 (2009).
[13] S. N. F. Zuikafly, W. M. F. Wan Nawawi, L. H. Ngee, H. Yahaya, W. J. Yahya, F. Ahmad, Journal of Physics: Conference Series **1371**, 012011 (2019).
[14] N. N. M. Rashid, H. Ahmad, M. F. Ismail, S. N. F. Zuikafly, N. A. Nordin, T. Koga, W. J. Yahya, H. Yahaya, F. Ahmad, Journal of Advanced Research in Micro and Nano Engineering **11**(1), 1 (2023).
[15] N. N. M. Rashid, M. Q. Lokman, S. N. F. Zuikafly, N. A. Nordin, H. Yahaya, M. F. Ismail, H. Ahmad, W. M. Fazli Wan Nawawi, F. Ahmad, Journal of Advanced Research in Applied Sciences and Engineering Technology **33**(1), 44 (2023).
[16] W. M. Fazli Wan Nawawi, K. Y. Lee, E. Kontturi, R. J. Murphy, A. Bismarck, ACS Sustainable Chemistry and Engineering **7**(7), 6492 (2019).
[17] G. Sobon, A. Duzynska, M. Świniarski, J. Judek, J. Sotor, M. Zdrojek, Scientific Reports **7**, 45491 (2017).
[18] K. Watanabe, Y. Zhou, Y. Sakakibara, T. Saito, N. Nishizawa, OSA Continuum **4**(1), 137 (2021).
[19] C. Gaillard, P. A. Stadelmann, C. J. G. Plummer, G. Fuchs, Scanning **26**, 122 (2004).
[20] S. N. Mohd Halim, F. Ahmad, M. Q. Lokman, H. H. J. Sapingi, M. F. Mohamad Taib, W. M. F. Wan Nawawi, H. Yahaya, M. A. A. Rahman, S. Shafie, S. W. Harun, Photonics **9**(10), 704 (2022).
[21] S. Z. Rogovina, C. V. Alexanyan, E. V. Prut, Journal of Applied Polymer Science **121**(3), 1850 (2011).
[22] N. Sazali, H. Ibrahim, A. S. Jamaludin, M. A. Mohamed, W. N. W. Salleh, M. N. Z. Abidin, IOP Conference Series: Materials Science and Engineering **788**, 012047 (2020).
[23] S. W. Harun, M. A. Ismail, F. Ahmad, M. F. Ismail, R. M. Nor, N. R. Zulkepely, H. Ahmad, Chinese Physics Letters **29**(11), 114202 (2012).

*Corresponding author: fauzan.kl@utm.my